JARQ 38 (2), 137 – 148 (2004) http://www.jircas.affrc.go.jp

An Evaluation of the Use of Integrated Spectral and Textural Features to Identify Agricultural Land Cover Types in Pangalengan, West Java, Indonesia

Ketut WIKANTIKA[1]*, Satoshi UCHIDA[2] and Yukiyo YAMAMOTO[2]

[1] Department of Geodetic Engineering, Institute of Technology Bandung (ITB) (Jl. Ganesha 10, Bandung 40132, Indonesia)
[2] Development Research Division, Japan International Research Center for Agricultural Sciences (JIRCAS) (Tsukuba, Ibaraki 305–8686, Japan)

Abstract

The objective of the study is to evaluate the use of integration of spectral and textural features derived from IKONOS imagery to identify agricultural land cover types in a mountainous case study area in Pangalengan, West Java, Indonesia. The study includes image preprocessing, development of an image quantization method, calculation of textural measures, development of data sets and an accuracy assessment. Image preprocessing focuses on image registration and topographic normalization. Topographic normalization is conducted to minimize the effect of illumination differences on surface reflectance. In this study, two image quantization methods, i.e. image segmentation and averaging filtered were developed. The image segmentation method classifies the image into several segmentations based on a determination of the total number of pixels per class, while the averaging filtered method classifies the image based on the average of the digital number values within a window size. Four textural measures, inverse difference moment, contrast, entropy and energy, were calculated based on the gray level co-occurrence matrix (GLCM). The results indicate that a combination of spectral and textural aspects significantly improves the classification accuracy compared with classification with pure spectral features only. Image segmentation and averaging filtered methods can reveal more effectively spatial forms of agricultural land cover types than using a 256 gray-level scale. The overall accuracy increased 11.33% when using the integration of spectral and multiple textural features of inverse difference moment (5×5) and energy (9×9).

Discipline: Information technology
Additional key words: land cover classification, image quantization, IKONOS

Introduction

Texture is an important characteristic for the analysis of many types of images such as an image obtained from aircraft or satellite platforms. It is the visual effect, which is produced by spatial distribution of tonal variations over relatively small areas[2]. The concept of texture can be investigated through its relationship with spectral data; in fact, textural and spectral information can both be present in an image or either one can dominate the other.

Many researches have investigated the extraction of textural features for mapping urban environments and land use classification using neural networks[1], several filtering methods[3,8,18,21,22,26,27], local standard deviation and autocorrelation[10], principal component and filtering[13], multitemporal SAR data[14], morphological processing[12,23], and image segmentation[7,14,20]. Their studies show that the integration of spectral and textural features improve the classification accuracy.

The objective of this study is to clarify the role of integration of spectral and textural features derived from IKONOS imagery for classification of agricultural land cover types in a mountainous case study area of Pangalengan, West Java, Indonesia. Two image quantization methods were developed to calculate textural features. Four textural measures, i.e. inverse difference moment, contrast, entropy, and energy were applied based on gray level co-occurrence matrix (GLCM). The maximum likelihood classification algorithm was used to classify land cover types of the study area and finally more than 280 data sets were assessed.

*Corresponding author: fax +62–22–2530702; e-mail ketut@gd.itb.ac.id
Received 5 August 2002; accepted 3 December 2003.

Study site

This study was conducted in a part of one of the villages in Pangalengan sub-district, Margamekar Village, in the south of Bandung, West Java, Indonesia, roughly between longitudes 107° 25'–107° 40' E and latitudes 7° 5'–7° 20' S, measuring approximately 13.45 km^2 (Fig. 1). The climate of the study area is humid tropical with annual precipitation averaging 1,250 mm every year[28]. Generally, the highest rainfall consistently occurs between December and March, and the lowest rainfall occurs between July and August. The topography is generally classified into 3 classes; flat to mildly undulating (29%), undulating to hilly (33%), and hilly to mountainous (38%). Elevation varies from 1,365 to 1,550 m above mean sea level. The major land cover types are residential, lake water, fallow land, vegetables, and tea plantation. Cabbage, potato and tomato are dominant vegetable types of the study area, while tea plantation covers more than 30% of the total study area.

Data

An IKONOS satellite image is the main data used in the study. Table 1 shows the specification of the data. Other data are a digital elevation model (DEM) with grid size of 50 m collected for preprocessing and other image analysis.

Methods

1. Preprocessing data

Image preprocessing focuses on geometric correction and topographic normalization. The IKONOS image was projected onto a Universal Transverse Mercator (UTM) with WGS 84 datum corresponding to other geographic data such as administrative boundaries and DEM data. Topographic slope may introduce radiometric distortion of the recorded signal[19]. In some locations, the area of interest might even be in complete shadow, dramatically affecting the brightness values of the pixels involved (i.e. spectral reflectance)[11]. Therefore it is important to reduce or remove topographic effects, especially in mountainous areas. In this study, the study area was assumed to be a lambertian reflectance model, this means that the surface reflected incident solar energy uniformly in all directions, and that variations in reflectance were due to the amount of incident radiation. To minimize the effect of illumination differences on the surface reflectance in mountainous areas, the digital number of spectral bands was calibrated using a normalized brightness equation[4]. This equation needed the information of sun azimuth and elevation at the time of image acquisition, DEM and the original image.

2. Spectral reflectance measurement

In this study, characteristics of spectral reflectance of land cover such as canopies of different vegetables, tea plantation and fallow land were measured using a portable photometer type 2703. The objective of this work is to select an appropriate spectral band of the IKONOS image for textural extraction. The spectral intervals of the photometer are 25 nm (400 to 675), 50 nm (700 to 750) and 100 nm (750 to 1,050). Several measurements were conducted while each measurement was collected twice and afterwards the average observation was calculated. All measurements were carried out in daytime under clear atmospheric conditions. Fig. 2 shows the characteristics of spectral reflectance profiles for tomato, long chili, tea plantation, fallow land, cabbage, and potato. In this case, the coverage condition of fallow land shows no vegetation cover on its surface.

According to the spectral reflectance profiles in Fig. 2, tomato, long chili, cabbage, and potato were classified into a united vegetable class. The spectral reflectance values of this class were fairly low ranging from 0 to 10% in the visible region. These spectral reflectance profiles correspond to spectral signatures extracted from the corrected IKONOS image.

3. Image quantization

The gray level number is an important factor in the computation of GLCM. Therefore, in this study, the

Table 1. IKONOS data specifications

Sensor	Spectral bands	Other specifications
IKONOS	Band-1/Blue: 0.45–0.52 μm Band-2/Green: 0.52–0.60 μm Band-3/Red: 0.63–0.69 μm Band-4/NIR: 0.76–0.90 μm	Spatial resolution: 4 m Sun azimuth: 108.66° Sun elevation: 56.57° Overpass time: 10:30 a.m. Acquired on February 6, 2000 Processing level: Geo product

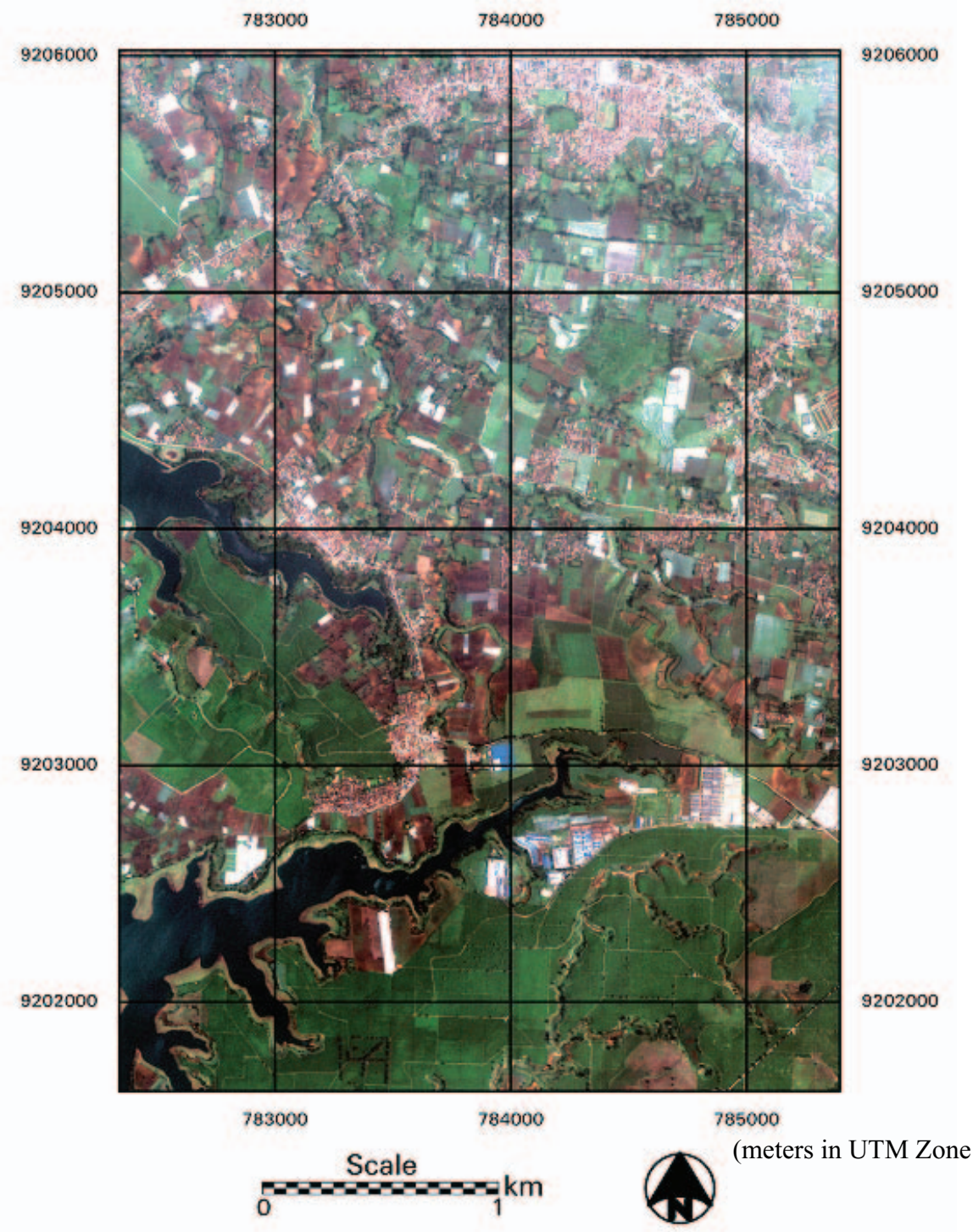

Fig. 1. Location of the study area, part of Margamekar Village

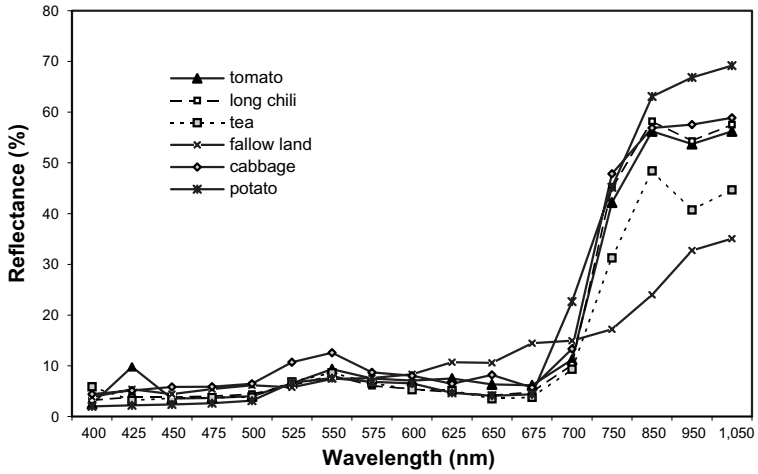

Fig. 2. Land cover spectral reflectance profiles measured by a portable photometer

commonly used method of image quantization, stored in a 256 gray level, and a proposed image quantization method; image segmentation and averaging filtered, were applied. The image segmentation method classifies the image into several segmentations based on the determination of total number of pixels per class, while the averaging filtered classifies the image based on the average of digital number values within a window size. For example, Fig. 3 shows image segmentation and averaging filtered results using the histogram of band 4 of IKONOS. Fig. 3A describes segmentation of the original 256 gray level image into 8 classes with class 1 ranging from digital number 0–39, class 2 from 40–58, class 3 from 59–77, class 4 from 78–98, class 5 from 99–119, class 6 from 120–138, class 7 from 139–153, and class 8 from 154–255. Fig. 3B and 3C show the result of the segmentation process and the histogram of the averaging filtered using window size of 3×3 pixels, respectively.

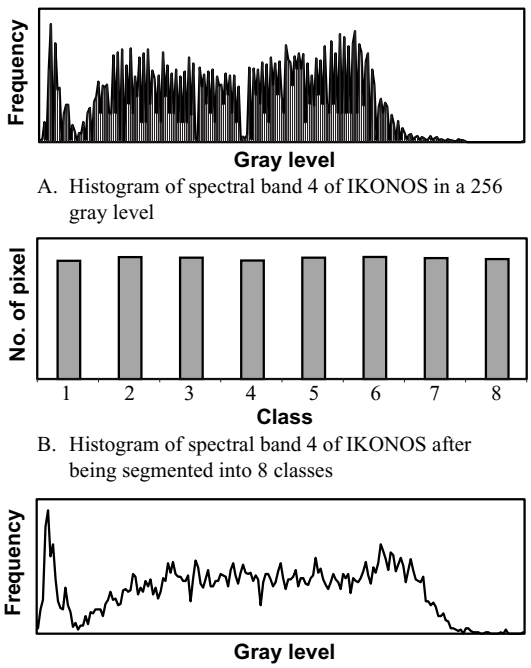

A. Histogram of spectral band 4 of IKONOS in a 256 gray level

B. Histogram of spectral band 4 of IKONOS after being segmented into 8 classes

C. Histogram of spectral band 4 of IKONOS after being averaged using window size of 3×3

Fig. 3. Example of image quantization using band 4 of IKONOS image

One image with a 256 gray level and 5 modified gray level images; 2 images developed from image segmentation and 3 images developed from averaging filtered with window sizes of 3×3, 5×5, and 7×7, were used to calculate textural information.

4. GLCM and textural measures

The commonly used method to calculate textural information is based on GLCM (gray level co-occurrence matrix). The definition of GLCMs is as follows[9]. Suppose an image to be analyzed is rectangular and has N_x resolution cells in the horizontal direction and N_y resolution cells in the vertical direction. Suppose that the gray tone appearing in each resolution cell is quantized to N_g levels. Let $L_x = \{1, 2, ..., N_x\}$ be the horizontal spatial domain, $L_y = \{1, 2, ..., N_y\}$ be the vertical spatial domain, and $G = \{1, 2, ..., N_g\}$ be the set of N_g quantized gray tones. The set $L_y \times L_x$ is the set of resolution cells of the image ordered by their row-column designations. The image I can be represented as a function, which assigns some gray tones in G to each resolution cell or pair of coordinates in $L_y \times L_x$; I: $L_y \times L_x \rightarrow G$. The texture-context information is specified by the matrix of relative frequencies $P(i,j)$ with two neighboring pixels separated by a distance d occurring on the image, one with gray level i and the other with gray level j.

Four texture measures were applied in this study; inverse difference moment, contrast, entropy, and energy[2,12,15,17,24,25,27]. Inverse difference moment is alternatively called homogeneity. Inverse difference moment is calculated using the following equation:

Inverse difference moment

$$= \sum_{i=1}^{N_g} \sum_{j=1}^{N_g} \frac{1}{1+(i-j)^2} P(i,j) \quad (1)$$

Contrast is the difference between the highest and the lowest values of a continuous set of pixels. Contrast is calculated using the following equation:

$$Contrast = \sum_{i=1}^{N_g} \sum_{j=1}^{N_g} (i-j)^2 P(i,j) \quad (2)$$

Entropy measures the disorder of an image. When the image is not texturally uniform, entropy is very large. Entropy is calculated using the following equation:

$$Entropy = -\sum_{i=1}^{N_g} \sum_{j=1}^{N_g} P(i,j) \log(P(i,j)) \quad (3)$$

Energy is also called the angular second moment or uniformity. Energy is calculated using the following equation:

$$Energy = \sum_{i=1}^{N_g} \sum_{j=1}^{N_g} (P(i,j))^2 \quad (4)$$

In this study, 12 window sizes of 3×3, 5×5, 7×7, ... 21×21, 23×23, 25×25 pixels were tested. The interpixel distance in the co-occurrence matrix calculation was one and the average of the 4 main interpixel angles was used for the computations. The textural features were obtained by using band 4 of the IKONOS image. The reason for choosing band 4 for computing textural features was due to the fact that this band had maximum variability in terms of standard deviation and range of gray level values compared with the other 3 bands. In addition, band 4 covers the near infrared which is useful for determining vegetation types and vigor, biomass content, and delineating water bodies[16]. These characteristics can be beneficial to classify the land cover types over the study area.

Results and discussion

Fig. 4 shows a portion of the study area in a 256 gray level (A), segmented into 4 classes (B) and 8 classes (C), and averaging filtered using window sizes of 3×3, 5×5, and 7×7 (D, E, F), respectively. Fallow land, which is indicated by the area with a white border, was classified into the same segment with the water feature, in the case of B. But the performance of the segment class was different when the whole image segmented into 8 classes (C), where the fallow land consists of 2 segments, i.e. segments with gray level values of 0–39 and 40–58. The

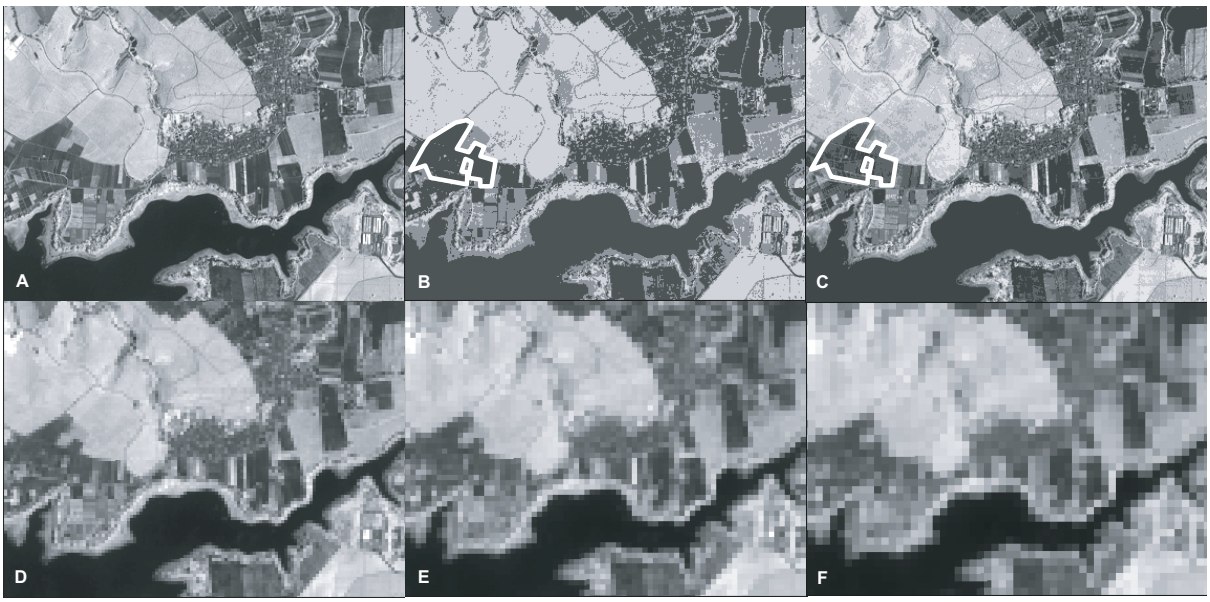

Fig. 4. Input images for textural features calculation
A: a 256 gray level, B: image segmentation in 4 classes, C: image segmentation in 8 classes, D: averaging filtered with 3×3 pixels, E: averaging filtered with 5×5 pixels, F: averaging filtered with 7×7 pixels.

gray level value of the whole image was averaged using window sizes of 3×3, 5×5, and 7×7 pixels as shown in Fig. 4D, E, and F, respectively. The figures show that the performance of the spectral visualization is different from each other.

Fig. 5 shows examples of textural features calculated from a 256 gray level (A, B, C, D) and segmented image (E, F, G, H) of band 4 of IKONOS. There were calculated 288 textural features. The 355 data sets were made consisting of one data set developed only using spectral bands 1, 2, 3, and 4 of the IKONOS image, 288 data sets were developed using a combination of single textural feature and all bands, and 66 data sets were developed using a combination of multiple textural features and all bands. All data sets were used to classify land cover into 5 classes, i.e. water, fallow land, vegetable field, tea plantation and residential areas using a maximum likelihood classification algorithm[16]. Accuracy assessment was conducted to compare the classification result with the reference data that were assumed to be true. In other words, the accuracy assessment determines the quality of the information derived from remotely sensed data. It can be quantitative with the purpose of identifying and measuring map errors[6]. It has been shown that more than 250 reference pixels are required to estimate the accuracy of a class within plus or minus 5%[5]. In this study, 400 reference pixels were collected to assess the accuracy of land cover classes over the study area.

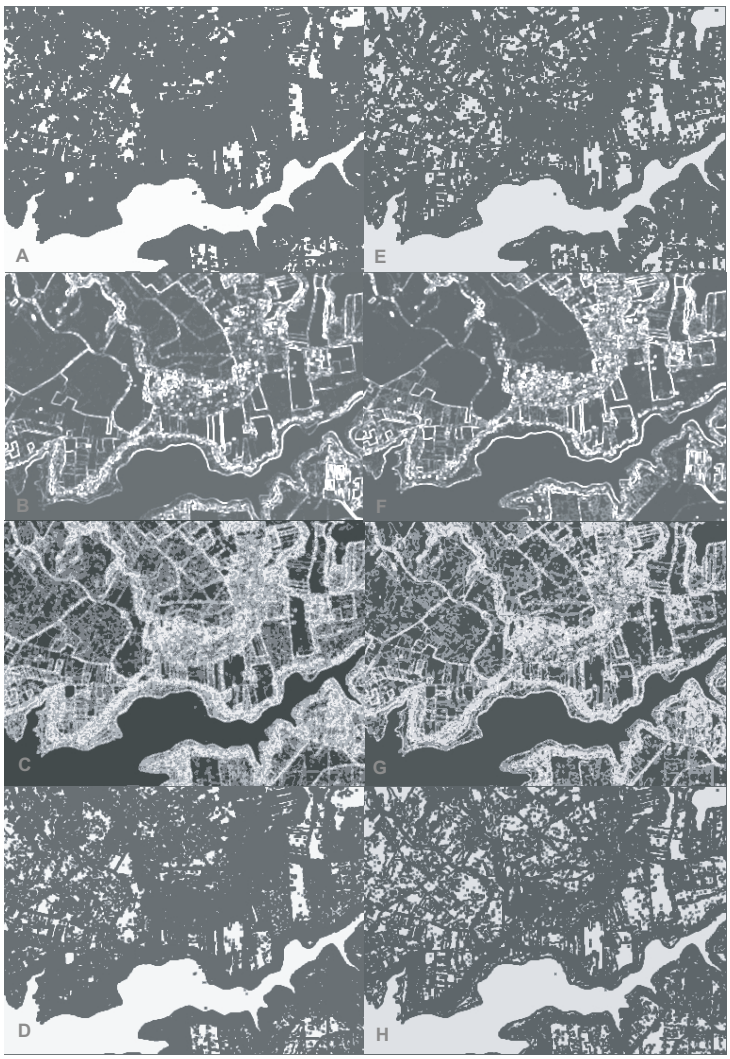

Fig. 5. Textural features derived from a 256 gray level image (A, B, C, D) and segmented image in 8 classes (E, F, G, H) with window size of 3×3
A & E: inverse difference moment, B & F: contrast, C & G: entropy, D & H: energy.

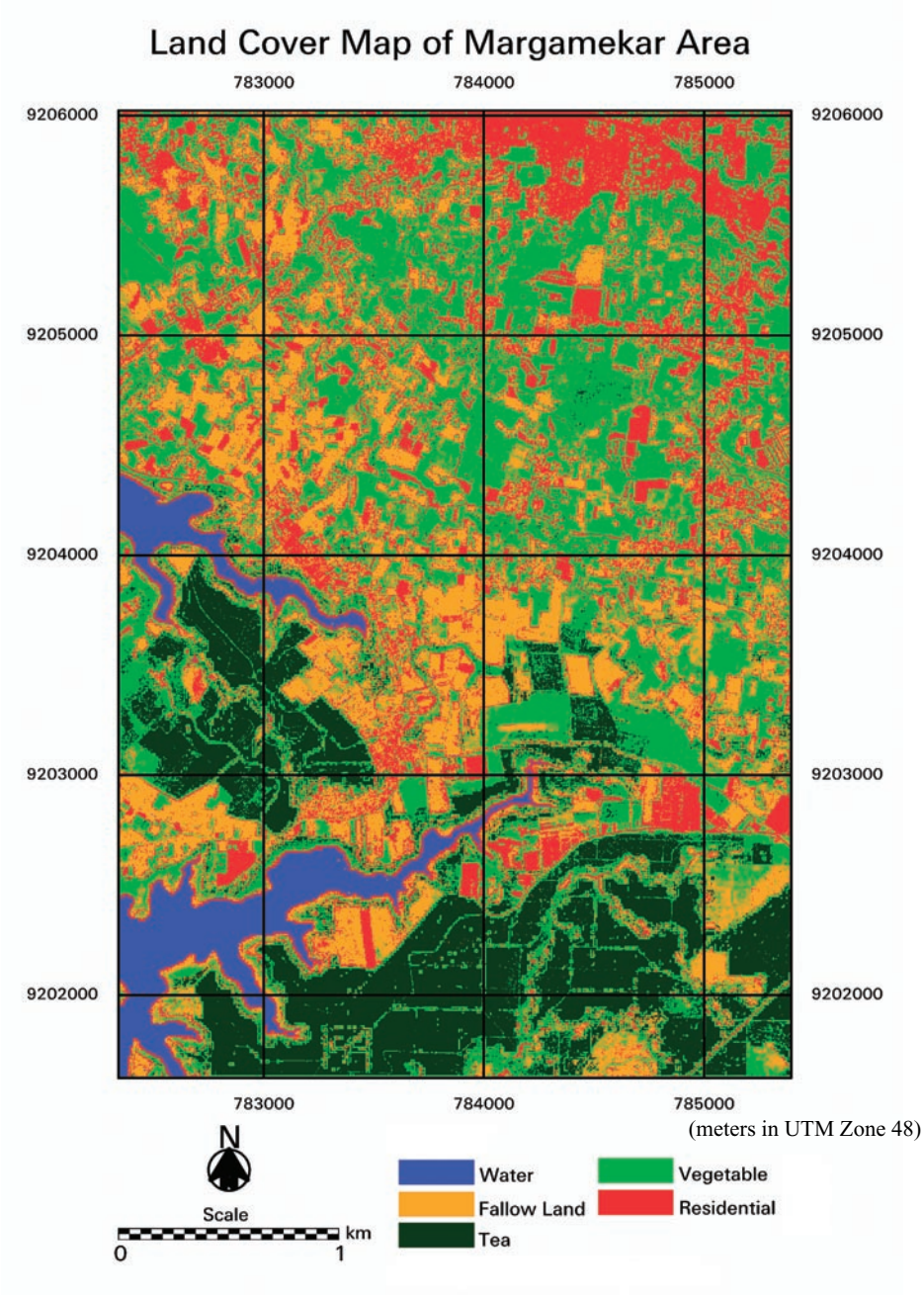

Fig. 6. Classification result only using spectral feature of IKONOS image

Table 2. The error matrix of classification result using spectral feature only

Classified as	Reference data					
	Water	Fallow	Tea	Vegetable	Residential	**Total**
Water	**15**	1	1	1	0	18
Fallow	1	**67**	2	10	10	90
Tea	0	2	**55**	10	1	68
Vegetable	1	6	3	**124**	13	147
Residential	2	6	2	9	**58**	77
Total	19	82	63	154	82	**400**

The overall accuracy is calculated with (15 + 67 + 55 + 124 + 58) / 400 = 79.75%

Table 3. The overall accuracy of classification results (%) using single texture feature

No.	Texture window size	Image quantization method					
		A 256 gray level	Segmentation		Averaging filtered		
			4 classes	8 classes	3×3	5×5	7×7
	IDM						
1	3×3	86.57	87.43	89.71	90.29	89.43	89.43
2	5×5	81.14	87.43	80.57	88.86	88.57	90.86
3	7×7	78.29	80.86	78.00	86.86	90.57	90.51
4	9×9	77.71	79.14	77.43	86.29	89.14	90.86
5	11×11	79.43	78.00	80.86	79.71	79.50	89.75
6	13×13	81.43	78.28	80.86	79.71	80.50	90.00
7	15×15	81.71	78.57	81.43	79.71	80.75	80.00
8	17×17	84.29	80.86	83.71	83.71	81.71	81.72
9	19×19	86.57	80.86	86.57	83.43	82.57	83.71
10	21×21	88.28	81.71	88.00	84.86	86.00	86.29
11	23×23	88.28	81.43	88.00	86.00	87.71	88.29
12	25×25	88.00	82.00	87.43	88.00	88.00	88.00
	CON						
13	3×3	82.86	87.14	83.71	82.86	89.71	90.00
14	5×5	79.43	87.14	79.71	83.14	86.86	90.57
15	7×7	80.57	85.71	80.27	87.43	87.14	89.43
16	9×9	80.00	86.00	81.71	86.57	86.57	89.14
17	11×11	82.86	86.00	82.57	87.14	85.75	89.75
18	13×13	83.43	85.71	81.14	87.14	85.75	88.50
19	15×15	83.71	86.00	82.86	86.75	87.50	89.00
20	17×17	85.14	87.43	82.29	87.43	88.29	87.71
21	19×19	85.71	87.14	82.00	88.57	88.00	88.57
22	21×21	85.71	86.29	82.86	88.57	87.14	88.86
23	23×23	85.43	86.86	82.58	88.29	86.29	88.86
24	25×25	85.43	86.86	82.29	87.14	87.43	88.29
	ENT						
25	3×3	87.71	88.00	88.86	88.57	89.71	88.86
26	5×5	87.43	85.43	88.57	87.43	89.43	88.57
27	7×7	86.57	85.71	87.71	86.86	90.00	88.86
28	9×9	84.28	86.00	86.00	88.00	88.86	87.71
29	11×11	86.00	86.57	86.00	87.25	88.00	90.25
30	13×13	87.43	86.29	86.29	88.75	89.25	90.50
31	15×15	86.86	86.00	84.86	89.75	89.50	90.75
32	17×17	89.43	87.71	87.43	88.29	89.14	90.00
33	19×19	89.43	86.57	87.43	87.14	89.14	90.00
34	21×21	88.00	86.87	87.43	87.43	88.86	88.29
35	23×23	88.00	87.43	87.43	88.00	89.14	87.43
36	25×25	88.00	89.14	86.86	87.71	90.00	88.00
	ENE						
37	3×3	88.00	87.14	88.57	90.29	89.43	89.14
38	5×5	81.71	86.29	88.00	89.71	88.86	89.14
39	7×7	82.29	84.29	87.14	89.14	88.57	88.86
40	9×9	82.29	86.00	81.14	88.29	89.43	90.29
41	11×11	80.57	86.86	79.43	86.25	89.25	90.00
42	13×13	79.71	86.86	78.57	85.00	89.00	90.00
43	15×15	79.43	87.43	78.29	82.75	88.50	89.25
44	17×17	81.14	88.00	80.86	80.29	82.29	89.14
45	19×19	80.86	86.57	80.86	80.57	81.43	88.29
46	21×21	81.71	86.86	80.57	81.14	80.86	87.71
47	23×23	81.43	86.86	81.14	81.43	81.43	88.00
48	25×25	81.14	86.00	80.29	81.14	81.43	88.00

IDM: inverse difference moment, CON: contrast, ENT: entropy, ENE: energy.

The overall classification accuracy of pure spectral bands of IKONOS was 79.75% (Fig. 6). The error matrix of this classification is listed in Table 2. Table 3 shows the overall classification accuracies using the combination of spectral and single textural features derived from IKONOS. This table indicates that combining the spectral and single textural features gives better accuracy than using only the spectral images. Quantization of the image with averaging filtered windows of 7×7 pixels provides better overall classification accuracy than the others, which ranges from 88–90%. The use of entropy in all window sizes and spectral features improves the overall classification accuracies more than using spectral features only. The overall classification accuracies with window sizes larger than 15×15 do not improve significantly for contrast (a 256 gray level, segmentation in 8 classes, averaging filtered with window size of 7×7), entropy (segmentation in 8 classes), or energy (segmentation in 4 and 8 classes). The residential class, which is relatively more heterogeneous than the other classes, has the optimal window size of 3×3 pixels. The tea plantation class has the optimal window size of 3×3 to 15×15 pixels.

Classification with multiple textural features was also conducted. The classification results for selected textural features showed high overall classification accuracy in Table 3. Table 4 indicates that an increase in the number of textural features does not contribute to increasing the classification accuracy. In the case of image segmentation for 8 classes, the integrated multiple textural features of inverse difference moment and energy provided the highest classification accuracy of 88.75%, which is not significantly different from using a single textural feature (Tables 3 and 5). However, the highest

Table 4. The overall accuracy of classification results using multiple textural features for a 256 gray level

No.	Data set	Texture	Overall accuracy (%)
1	Using 2 textures	IDM + CON	83.25
2		IDM + ENT	85.75
3		IDM + ENE	85.50
4		CON + ENT	83.75
5		CON + ENE	82.00
6		ENT + ENE	84.50
7	Using 3 textures	IDM + CON + ENT	83.25
8		IDM + CON + ENE	81.50
9		IDM + ENT + ENE	83.00
10		CON + ENT + ENE	81.50
11	Using 4 textures	IDM + CON + ENT + ENE	80.50

IDM: inverse difference moment, CON: contrast, ENT: entropy, ENE: energy.

Table 5. The overall accuracy of classification results using multiple textural features for image segmentation

No.	Data set	Texture	Overall accuracy (%)	
			4 classes	8 classes
1	Using 2 textures	IDM + CON	84.00	81.75
2		IDM + ENT	85.25	86.50
3		IDM + ENE	84.25	88.75
4		CON + ENT	84.25	82.50
5		CON + ENE	85.25	81.50
6		ENT + ENE	85.75	86.25
7	Using 3 textures	IDM + CON + ENT	82.75	80.75
8		IDM + CON + ENE	83.75	82.25
9		IDM + ENT + ENE	83.75	85.75
10		CON + ENT + ENE	84.25	80.25
11	Using 4 textures	IDM + CON + ENT + ENE	83.50	80.50

IDM: inverse difference moment, CON: contrast, ENT: entropy, ENE: energy.

Table 6. The overall accuracy of classification results using multiple textural features for averaging filtered

No.	Data set	Texture	Overall accuracy (%)		
			3×3	5×5	7×7
1	Using 2 textures	IDM + CON	86.25	87.50	88.25
2		IDM + ENT	88.50	88.75	89.50
3		IDM + ENE	90.50	89.00	91.00
4		CON + ENT	87.00	87.50	89.75
5		CON + ENE	85.75	90.00	88.00
6		ENT + ENE	88.25	88.25	90.50
7	Using 3 textures	IDM + CON + ENT	86.75	86.50	87.75
8		IDM + CON + ENE	85.75	87.75	87.75
9		IDM + ENT + ENE	88.25	88.00	90.00
10		CON + ENT + ENE	86.50	87.25	89.00
11	Using 4 textures	IDM + CON + ENT + ENE	86.00	86.25	88.75

IDM: inverse difference moment, CON: contrast, ENT: entropy, ENE: energy.

Table 7. The best overall accuracy of classification results for each image quantization method using single and multiple textural features

No.	Image quantization	Texture (window size)		Overall accuracy (%)	
		Single	Multiple	Single	Multiple
1	A 256 gray level image	ENT(17×17)	IDM(21×21) + ENT(17×17)	89.43	85.75
2	Image segmentation (8 classes)	IDM(3×3)	IDM(3×3) + ENE(17×17)	89.71	88.75
3	Averaging filtered (7×7)	IDM(5×5)	IDM(5×5) + ENE(9×9)	90.86	91.00

IDM: inverse difference moment, ENT: entropy, ENE: energy.

Table 8. The error matrix of the best classification result using spectral and textural features

Classified as	Reference data					
	Water	Fallow	Tea	Vegetable	Residential	**Total**
Water	**19**	0	0	0	0	19
Fallow	0	**74**	2	4	5	85
Tea	0	0	**59**	4	1	64
Vegetable	0	4	2	**140**	4	150
Residential	0	4	1	5	**72**	82
Total	19	82	64	153	82	**400**

The overall accuracy is calculated with (19 + 74 + 59 + 140 + 72) / 400 = 91.00%

classification accuracy of 91% was achieved when using the inverse difference moment (5×5) and energy (9×9) from an averaging filtered image with window size of 7×7 (Table 6). Table 7 shows the best overall accuracy of classification results for each image quantization method using single and multiple textural features. Fig. 7 is the overall classification result of 91% using integration of spectral and multiple textural features (Table 7, No. 3). This combination improved significantly individual classification results of fallow land and residential classes compared with only using spectral features. Table 8 shows the error matrix of the best classification result.

It can be explained that a pair class of fallow land and residential areas contributed to misclassification of class mixtures, therefore individual accuracy of these classes were lower than other classes. However, these classes have been improved using integration of spectral and textural features, with single or multiple features.

Conclusions

This study demonstrated the effect of integration of

spectral and textural features on classification accuracy of agricultural land cover types in a mountainous area in Pangalengan, West Java, Indonesia, using IKONOS imagery. The following conclusions were obtained.

(1) The use of integrated spectral and textural features improved the classification accuracy more than in the

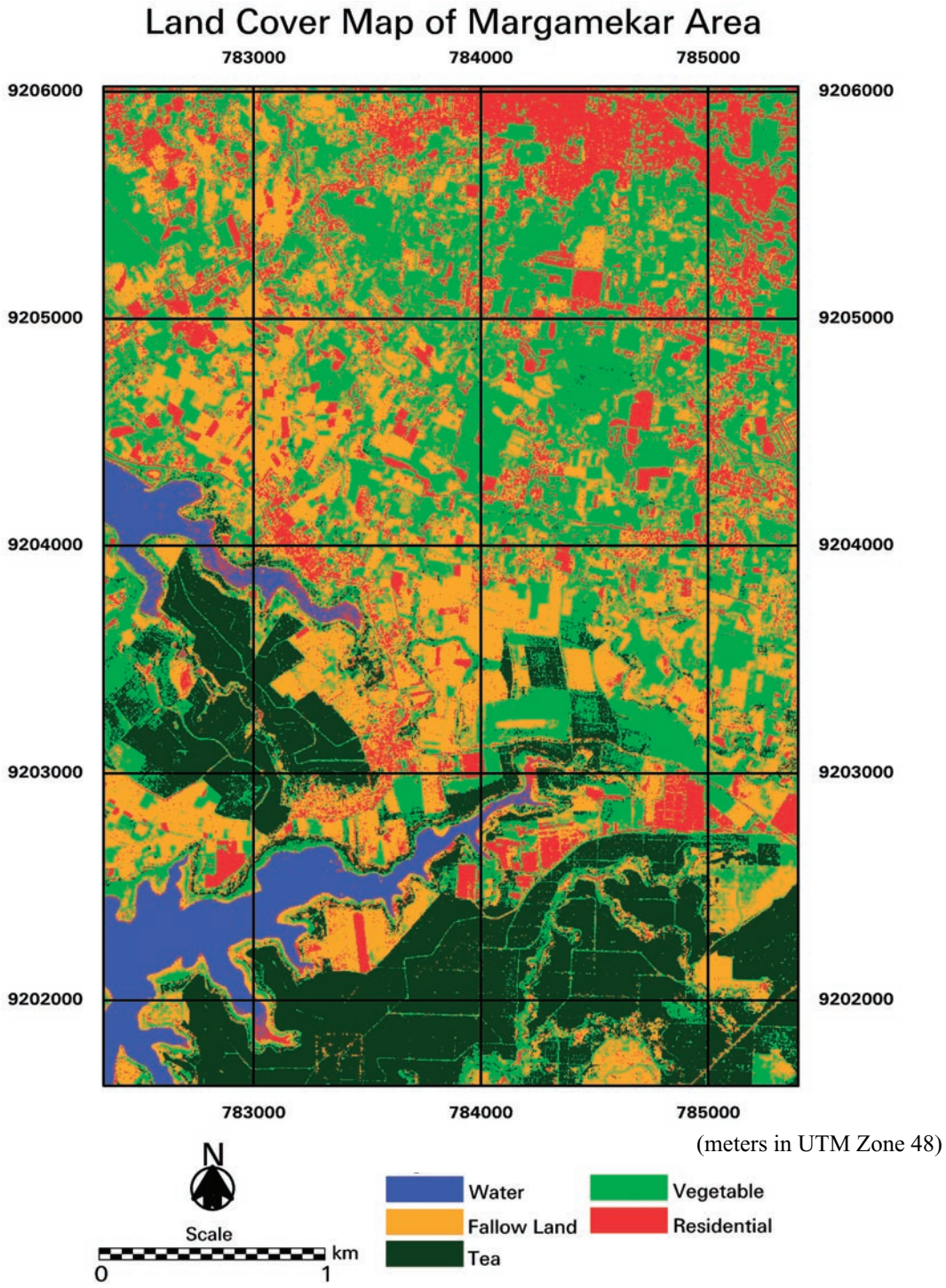

Fig. 7. The best classification result using spectral and textural features of inverse difference moment (5×5) and energy (9×9)
Image quantization used is averaging filtered with 7×7.

case of using spectral analysis only.

(2) Increase in the size of the window (from 3×3 to 15×15 pixels) improved the overall accuracy up to a certain limit. For all the features, the optimal window size was identified to be between 5×5, 7×7, and 9×9 pixels. Increase of window size beyond this showed no significant contribution to improving accuracy of classification.

(3) The proposed image quantization methods brought an improvement of providing better overall classification accuracies than using a 256 gray level image.

References

1. Bandibas, J. C. (1998) Combining the spectral and spatial signatures of information classes using artificial neural network based classifier for remote sensing of spatially heterogeneous land use/land cover systems in tropics. *In* Proc. 19th Asian Conf. Remote Sens., Asian Association on Remote Sensing, Manila, Philippine, 121–127.
2. Baraldi, A. & Parmiggiani, F. (1995) An investigation of the textural characteristics associated with gray level cooccurrence matrix statistical parameters. *IEEE Trans. Geosci. Remote Sens.*, **33**(2), 293–304.
3. Beauchemin, M., Thomson, K. P. B. & Edwards, G. (1996) Edge detection and speckle adaptive filtering for SAR images based on a second-order textural measure. *Int. J. Remote Sens.*, **17**(9), 1751–1759.
4. Colby, D. (1991) Topographic normalization in rugged terrain. *Photo. Eng. Remote Sens.*, **57**(5), 531–537.
5. Congalton, R. (1991) A review of assessing the accuracy of classifications of remotely sensed data. *Remote Sens. Environ.*, **37**, 35–46.
6. Congalton, R. & Green, K. (1999) Assessing the accuracy of remotely sensed data; principles and practices. Lewis Publishers, Boca Raton, pp.137.
7. Conners, R. W., Trivedi, M. M. & Harlow, C. A. (1984) Segmentation of a high-resolution urban scene using texture operators. *Comput. Vision Graph. Image Proc.*, **25**, 273–310.
8. Dutra, L. V. & Nelson, D. A. M. (1984) Some experiments with spatial feature extraction methods in multispectral classification. *Int. J. Remote Sens.*, **5**(2), 303–313.
9. Haralick, R. M., Shanmugam, K. & Dinstein, I. (1973) Textural features for image classification. *IEEE Trans. Sys. Manage. Cybernetics*, **SMC-3**(6), 610–621.
10. Horgan, G. W. et al. (1992) Land use classification in central Spain using SIR-A and MSS imagery. *Int. J. Remote Sens.*, **13**(15), 2839–2848.
11. Jensen, J. R. (1996) Introductory digital image processing; a remote sensing perspective. Prentice Hall Inc., N.J., pp.316.
12. Karathanassi, V., Iossifidis, C. H. & Rokos, D. (2000) A texture-based classification method for classifying built areas according to their density. *Int. J. Remote Sens.*, **21**(9), 1807–1823.
13. Kuplich, T. M., Freitas, C. C. & Soares, J. V. (2000) The study of ERS-1 SAR and Landsat TM synergism for land use classification. *Int. J. Remote Sens.*, **21**(10), 2101–2111.
14. Kurosu, T. et al. (1999) Texture statistics for classification of land use with multitemporal JERS-1 SAR single-look imagery. *IEEE Trans. Geosci. Remote Sens.*, **37**(1), 227–235.
15. Kushwaha, S. P. S., Kuntz, S. & Oesten, G. (1994) Applications of image texture in forest classification. *Int. J. Remote. Sens.*, **15**(11), 2273–2284.
16. Lillesand, T. M. & Kiefer, R. W. (1994) Remote sensing and image interpretation. John Wiley & Sons, New York, pp.750.
17. Marceau, D. J. et al. (1990) Evaluation of the gray level co-occurrence matrix method for land cover classification using SPOT. *IEEE Trans. Geosci. Remote Sens.*, **28**(4), 513–519.
18. Gong, P., Marceau, D. J. & Howarth, P. J. (1992) A comparison of spatial feature extraction algorithms for land-use classification with SPOT HRV data. *Remote Sens. Environ.*, **40**, 137–151.
19. Proy, C., Tanre, D., & Deschamps, P. Y. (1989) Evaluation of topographic effects in remotely sensed data. *Remote Sens. Environ.*, **30**, 31–32.
20. Ryherd, S. & Woodcock, C. (1996) Combining spectral and texture data in the segmentation of remotely sensed images. *Photo. Eng. Remote Sens.*, **62**(2), 181–193.
21. Shaban, M. A. & Dikshit, O. (1999) Land use classification for urban areas using spatial properties. *In* Int. Geosci. Remote Sens. Symp. (IGARRS), Hamburg, Germany, 1140–1142.
22. Shaban, M. A. & Dikshit, O. (2001) Improvement of classification in urban areas by the use of textural features; the case study of Lucknow city, Uttar Pradesh. *Int. J. Remote. Sens.*, **22**(4), 565–593.
23. Smits, P. C. et al. (1998) Multi-temporal analysis of urban areas using textural information in space-borne imagery. *In* Int. Geosci. Remote Sens. Symp. (IGARRS), Seattle, Washington, USA, 2580–2582.
24. Soares, J. V. et al. (1997) An investigation of the selection of texture features for crop discrimination using SAR imagery. *Remote Sens. Environ.*, **59**, 234–247.
25. Soh, L. K. & Tsatsoulis, C. (1999) Texture analysis of SAR sea ice imagery using gray level co-occurrence matrices. *IEEE Trans. Geosci. Remote Sens.*, **37**(2), 780–795.
26. Toll, D. (1985) Analysis of digital Landsat-MSS and SEASAT SAR data for use in discriminating land cover at the urban fringe of Denver, Colorado. *Int. J. Remote Sens.*, **6**(7), 1209–1229.
27. Zhang, Y. (1999) Optimization of building detection in satellite images by combining multispectral classification and texture filtering. *ISPRS J. Photo. Remote Sens.*, **54**, 50–60.
28. Data monografi kecamatan (2001) Kecamatan Pangalengan, Bandung, Jawa Barat.